ORIGINAL PAPER

Enhanced detection of olefins using ambient ionization mass spectrometry: Ag$^+$ adducts of biologically relevant alkenes

Ayanna U. Jackson · Thomas Shum · Ewa Sokol ·
Allison Dill · R. Graham Cooks

Abstract Spray solvent doped with silver ions increases the ease of olefin detection by desorption electrospray ionization (DESI). Characteristic silver adducts were generated in up to 50 times greater abundance when compared to conventional DESI spray solvents for the biologically significant olefin, arachidonic acid, in the positive ion mode. In the analysis of 26 lipids, silver adduct formation was highly favorable for fatty acids, fatty acid esters and prostaglandins but not applicable to some other classes (e.g., polar lipids such as ceramide and its derivative cerebroside sulfate). An investigation exploring competitive Ag$^+$ cationization with a mixture of components demonstrated that polyunsaturated compounds form Ag$^+$ adducts most readily. Silver cationization allowed the distinction between three sets of isomers in the course of multiple-stage collision-induced dissociation, so providing insight into the location of the olefin bonds. A silver ion-doped solvent was used in DESI imaging of normal and tumor canine bladder tissue sections. The Ag$^+$ fatty acid adducts permitted post facto differentiation between the normal and tumor regions. In addition, silver adduct formation in the course of DESI imaging of tissue sections revealed the presence of triacylglycerides, a class of compounds not previously identified through DESI imaging. A simple silver nitrate spray solvent has the potential to further improve DESI analysis of unsaturated biomolecules and other molecules containing π-bonds through selective silver cationization.

Introduction

Lipidomics is a growing field in which an understanding of the relative levels of lipids in the normal healthy state increases the possibility that detection of irregularities might provide useful information on the emergence of disease [1–5]. Polyunsaturated lipids such as arachidonic acid, squalene, and oxidized metabolites like prostaglandins and cholesterol, are essential to the diverse functionalities of the cell [1]. Unsaturated lipids are useful as biomarkers in diagnosis carried out on biological fluids and their identification and quantification usually requires extensive sample preparation and separation prior to mass spectrometric analysis. Ambient ionization methods [6–8], like desorption electrospray ionization (DESI) [9, 10], require minimal sample preparation and are potentially useful adjuncts to conventional methods of trace chemical analysis. These methods are normally applied to solid samples and they work best for polar analytes, so the low polarity of the unsaturated fatty acid chains means that the direct analysis of some lipids by ambient ionization mass spectrometry can be difficult.

Analysis of olefins by mass spectrometry has typically been confined to traditional ionization methods. These

A. U. Jackson · T. Shum · E. Sokol · A. Dill · R. G. Cooks (✉)
Department of Chemistry, Purdue University,
West Lafayette, IN 47907, USA
e-mail: cooks@purdue.edu

A. U. Jackson · T. Shum · E. Sokol · A. Dill · R. G. Cooks
Bindley Bioscience Center, Discovery Park, Purdue University,
West Lafayette, IN 47907, USA

 Springer

volatile compounds often are amenable to gas chromatography which commonly utilizes electron impact ionization (EI) or chemical ionization (CI). Chemical derivatization of more complex analytes is often needed prior to GC analysis in order to increase the volatility of the analyte or to change the functionality into groups that ionize more readily [11–16]. Electrospray ionization (ESI) and matrix-assisted laser desorption ionization typically require the presence of metal salts (often adventitious) to provide cations for simple charged adduct formation from olefins [17–22].

Silver ions form cationic adducts with several functional groups but demonstrate unusual affinity for olefinic compounds. This affinity is a result of the free $4d$ and $5s$ orbitals of the Ag^+ ion forming a partial bond with the $2p\pi$ orbitals of olefin bonds [23]. The formation of a weak charge-transfer silver adduct with the olefin groups of unsaturated molecules is particularly favored when two olefin groups are appropriately configured [24]. Silver ions also form adducts with aromatic species through pi-stacking interactions resulting in intermolecular chelation [23–25]. Silver ion interactions with olefins have been extensively studied using conventional chromatography [23, 26, 27], ESI-MS [17–19], and SIMS [24, 28, 29] but have not been explored for the direct analysis of olefins by ambient ionization methods.

DESI [9, 10] is an established ambient mass spectrometry ionization method for organic and biological compounds. The absolute sensitivity of DESI is typically on the order of low nanograms but much lower detection limits have been reported [30]. The reproducibility of the analysis is acceptable showing quantitation capabilities with relative standard deviations typically less than 20% and often much lower [31–35]. The mechanism of DESI ionization has been confirmed through experimental and computational studies: the process involves analyte dissolution followed by release from the surface in secondary microdroplets generated in the course of primary droplet impact [36–38]. DESI has been developed to include several variants including (1) non-proximate detection [39], (2) molecular imaging [40, 41], (3) derivatization accompanying ionization, a process referred to as reactive DESI [42, 43], and (4) analysis within a confined volume which is well-suited to high throughput experiments known as geometry independent DESI [44].

Here, silver ions are used in the direct analysis of unsaturated lipids in a method that increases the specificity of analysis of particular analytes by the generation of silver adducts. This approach was evaluated for 26 biologically relevant unsaturated lipids by adding trace amounts of silver nitrate to the DESI spray solvent. The experiment was further extended to DESI imaging, including attempted differential analysis of normal and malignant tissue.

Experimental

Standards and solvents

The compounds investigated are summarized in Electronic Supplementary Material Table S1. The fatty acids and their derivatives were obtained from Cayman Chemical (Ann Arbor, Michigan). The lipids and prostaglandin-E1 were purchased from Avanti Polar Lipids, Inc. (Alabaster, Alabama). Prostaglandin 8-iso-F2α was obtained from Alexis Biochemicals (Plymouth Meeting, PA). Research grade solvents, methanol (MeOH) and acetonitrile (ACN), from Mallinckrodt (Paris, KY) and water (Millipore Milli Q unit at 18.2 MΩ cm) were evaluated as DESI spray solvents with NaCl (Mallinckrodt, Paris, KY) and AgNO$_3$ (Mallinckrodt, Paris, KY) additives. Chloroform (research grade from Mallinckrodt, Paris, KY) and methanol or ethanol (Pharmco-AAPER, Brookfield, CT) was used to dilute the analytes from stock solutions for analysis.

Instrumental parameters

A Thermo Fisher Scientific LTQ (San Jose, CA) equipped with a linear ion trap was used for the experiments which were performed in the positive ion mode except when otherwise indicated. The typical instrumental parameters included: automatic gain control ON, 2 microscans, 200 ms maximum ion injection time, ±15 V capillary voltage, 150 °C capillary temperature, and ±65 V tube lens voltage. Identification of the analytes was confirmed using collision-induced dissociation. The experimental parameters for multiple-stage (MS^n) analysis, where $n=2$–5, varied but included an isolation window of 1.5–2.0 Th (Th, Thomson, mass/charge unit), collision energy 25–30% (manufacturer's unit), and 1 microscan with a maximum ion injection time of 100 ms. Data were acquired and processed using Xcalibur software (Thermo Fisher Scientific; San José, CA).

DESI experimental parameters

An OmniSpray™ ion source from Prosolia, Inc. (Indianapolis, IN) was used in these experiments. A spray angle of ~55° to the horizontal was used with the sample placed ~1–2 mm from both the MS inlet and the DESI spray source and with a take-off angle close to zero (relative to the horizontal). Typically, 3 μL solution of analyte was deposited onto a polytetrafluoroethylene (PTFE) substrate and allowed to dry prior to analysis in triplicate. The typical analyte spot had an area of ~7 mm^2 on the PTFE substrate. The entire spot was analyzed by rastering during the analysis. AgNO$_3$ (1–7 μg/mL)

solutions in MeOH:H_2O (1:1) were prepared daily from a concentrated stock or from the solid. Typical DESI parameters were used with regard to nebulizing gas, source voltage and solvent flow rate [9, 10].

DESI imaging parameters

DESI imaging experiments [33] were performed on canine bladder tissue sections to evaluate the application of the silver-doped spray to the analysis of lipid molecules within a biological matrix in the positive ion mode. Details for the preparation of the tissue samples can be found elsewhere [45]. A laboratory prototype DESI spray source was used for the imaging experiments on a homebuilt 2-D automated stage. An extended MS atmospheric inlet was used with a larger internal diameter than the standard commercial inlet, ~300–400 μm. The DESI spray source was optimized at an angle of 52°, ~2 mm from the sample surface and from the atmospheric inlet. A nitrogen gas pressure of 150 psi and solvent flow rate of 1.5 μL/min was used for the imaging experiments. The samples were scanned in horizontal rows separated by 200 μm vertical steps until the entire sample was assayed. Under the given DESI conditions, the spot size (diameter) was less than 250 μm. An in-house program enabled the conversion of the mass spectrometer manufacturer's Xcalibur 2.0 raw files into a format compatible with BioMap (freeware, http://www.maldi-msi.org) software. The individual pixel-by-pixel spectra or pixels acquired were assembled into a spatially accurate image using the BioMap software. The images were obtained using a spray solvent of pure acetonitrile doped with 5.5 μg/mL $AgNO_3$.

Results and discussion

Optimization of silver adduct formation during DESI

The doping of silver ions into the DESI spray solvent, in the form of $AgNO_3$, resulted in silver olefin adducts of fatty acids and their ester derivatives. The observed adducts are easily recognized by the characteristic 1:1 abundance ratio for the ^{107}Ag:^{109}Ag isotopes. When the concentration of $AgNO_3$ in the spray solvent was above 10 μg/mL (10 ppm), the mass spectrum was dominated by adducts of silver and nitrate ions with various solvent species. On the other hand, when the concentration of the silver salt was too low (below 1 μg/mL (<1 ppm)), silver cationization was not favored. An intermediate concentration of ~1–10 μg/mL of $AgNO_3$ in MeOH:H_2O (1:1) was ideal for formation of adducts with the analytes investigated. In the lower mass range (<200 Da) the spectra are still dominated by silver ion adducts of the solvent molecules. However, this is not a problem for the biological analytes of interest here.

Arachidonic acid was examined using common DESI spray solvents to perform an initial evaluation of the enhancement of signal that can be observed upon silver adduct formation. When arachidonic acid was analyzed using MeOH:H_2O (1:1), molecular ions were observed in the positive and negative ion full scan mass spectra at limits of detection of 150 ng and 30 ng, respectively. In the positive ion mode, the Na^+ adduct was typically observed while in the negative ion mode the deprotonated analyte, $[M–H]^-$, was observed. The limit of detection was also evaluated using MeOH:H_2O (1:1) with 100 μM NaCl, and it improved by an order of magnitude to 15 ng when monitoring the sodium adduct. The chloride adduct was not observed in the negative ion mode. A similar detection limit was achieved for the analysis of arachidonic acid when using a 2 μg/mL $AgNO_3$ ACN:MeOH (1:1) spray solvent but this improved to 3 ng when using MeOH:H_2O (1:1) and pure ACN spray solvents doped with 2 μg/mL $AgNO_3$. In the optimized solvent, the limit of detection was five times better than the best achieved for optimized sodium ion attachment and 50 times better than that achieved using the standard methanol/water solution in the positive ion mode. These results are summarized in Table 1.

Evaluation of silver cationization for biological compounds

The ability to form silver adducts was evaluated for additional fatty acids as well as their esters and also for other lipids (phospholipids, natural lipids, and prostaglandins). A total of 26 compounds varying in the structure, functional groups and the number of olefin groups were evaluated in the positive ion mode from a teflon substrate. Electronic Supplementary Material Table S1 summarizes and categorizes the different types of biomolecules. For an initial evaluation of silver's affinity for the different olefins, 3 ng of each analyte was analyzed. Only the fatty acids, their derivatives and the prostaglandins could be detected as silver ion adducts. While the phospholipids were not detected using these sample amounts, most of the phospholipids, such as 18:1

Table 1 Detection limit of arachidonic acid Ag^+ adducts using different spray solvents

Spray Solvent	Ionization Polarity	Detection Limit (ng)
MeOH:H_2O (1:1)	+	150
MeOH:H_2O (1:1)	−	30
100 μM NaCl MeOH:H_2O (1:1)	+	15
2 μg/mL $AgNO_3$ MeOH:H_2O (1:1)	+	3
2 μg/mL $AgNO_3$ ACN/MeOH (1:1)	+	15
2 μg/mL $AgNO_3$ ACN	+	3

PE (where PE refers to phosphoethanolamine) and C24:1 galactosyl ceramide, could be observed readily at higher concentrations (~100 μg/mL; 300 ng absolute). Cationization of ceramide, cerebroside and L-α-phosphatidylethanolamine of Electronic Supplementary Material Table S1 was not detected, even at higher concentrations (100–500 μg/mL; 300–1,500 ng absolute).

Figure 1 illustrates Ag$^+$ adduct formation with palmitoleic acid, linoleic acid, γ-linolenic acid and arachidonic acid which contain one, two, three, and four olefin bonds, respectively, each examined at 3 ng except for arachidonic acid, where 15 ng was analyzed. Based on the structures of the analytes and the ions observed, the molecules clearly complex with a single silver ion under these experimental conditions. In the case of structures with parallel *cis* olefins, it is not clear if the silver ion is bound to one or both olefins given that free rotation of the molecules is possible.

The successful detection of fatty acids by silver ion complexation raises the question of the selectivity of this reaction. To evaluate if Ag$^+$ adduct formation correlates to the number of olefin bonds present, the limit of detection of each of the fatty acids and their derivatives was determined. The limit of detection in this study was determined in the

full scan mass spectrum based on the corresponding isotopic profile of the Ag$^+$ (107:109 1.08:1.00) form of the molecular ion at a signal to noise ratio of 3. The identity of the ions measured was confirmed by tandem mass spectrometry (MS/MS). Overall, the limits of detection ranged from 1.5–3,000 pg (3 μL, ~3 mm sample spot of 1–1,000 ng/mL standard solutions) with no specific trend with respect to the number of olefin bonds, as summarized in Table 2. In general, the esters yielded lower detection limits than the free fatty acids, likely due to their increased basicity and hence increased cation affinity.

To further evaluate the signal in the Ag$^+$ ion/DESI experiment, all of the fatty acids and their derivatives were compared to the data collected using conventional DESI and ESI. Since fatty acids can also be detected in the negative ion mode, a comparison of the silver adduct detection limits to deprotonated ion detection limits was also made using a conventional DESI spray solvent, MeOH:H$_2$O (1:1). The detection limits of the silver adducts were typically at least an order of magnitude lower than those achieved using simple deprotonation. An additional comparison was made with electrosonic spray (ESSI) ionization [46], a technique similar to conventional electrospray ionization as the analyte
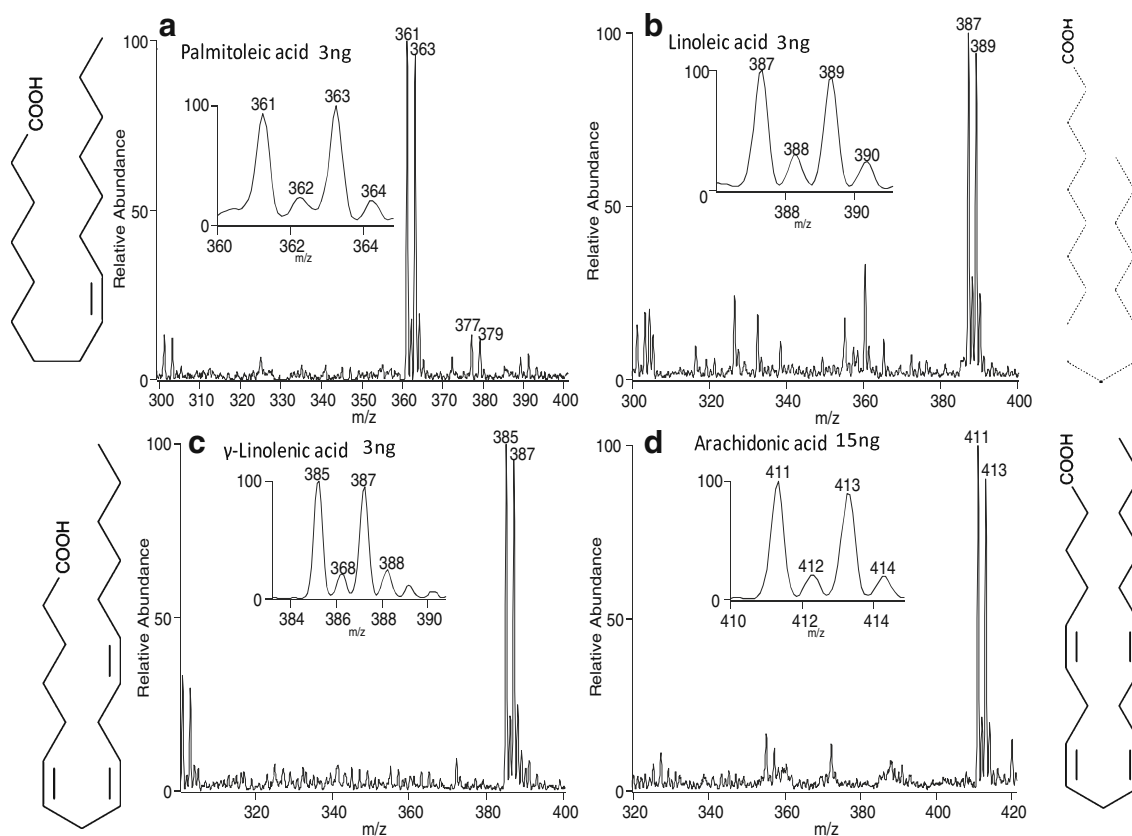

Fig. 1 DESI mass spectra of silver adducts examined from teflon using a solvent spray of MeOH:H$_2$O (1:1) doped with 5.5 μg/mL of AgNO$_3$ for **a** 3 ng of palmitoleic acid; **b** 3 ng of linoleic acid; **c** 3 ng of γ-linolenic acid; **d** 15 ng arachidonic acid analyzed using a Thermo Fisher Scientific LTQ of 3-μL pipetted samples (~7 mm^2 spot size)

Table 2 DESI Ag$^+$ adducts of biologically relevant analytes

Analyte (No. of Olefin Bonds)	Molecular Formula	m/z[a]	LOD (pg)
Fatty Acids and Esters			
Oleic acid (1)	$C_{18}H_{34}O_2$	389/391	30
Oleic acid ethyl ester (1)	$C_{20}H_{38}O_2$	417/419	3,000
Palmitoleic acid (1)	$C_{16}H_{30}O_2$	361/363	300
Palmitoleic acid ethyl ester (1)	$C_{18}H_{34}O_2$	389/391	3,000
Linoleic acid (2)	$C_{18}H_{32}O_2$	387/389	1,500
Linoleic acid ethyl ester (2)	$C_{20}H_{36}O_2$	415/417	3
γ-Linolenic Acid (3)	$C_{18}H_{30}O_2$	385/387	300
α-Linolenic acid (3)	$C_{18}H_{30}O_2$	385/387	3,000
Linolenic acid ethyl ester (3)	$C_{20}H_{34}O_2$	413/415	1.5
Pinolineic acid (3)	$C_{18}H_{30}O_2$	385/387	300
Pinolenic acid ethyl ester (3)	$C_{20}H_{34}O_2$	413/415	30
Arachidonic acid (4)	$C_{20}H_{32}O_2$	411/413	3,000
Arachidonic acid-d$_8$ (4)	$C_{20}H_{24}D_8O_2$	419/421	3,000
Arachidonic acid ethyl ester (4)	$C_{22}H_{36}O_2$	439/441	500
Arachidonic acid methyl ester (4)	$C_{21}H_{34}O_2$	425/427	3,000
Prostaglandins			
Prostaglandin E1 (1)	$C_{20}H_{34}O_5$	461/463	3,000
Prostaglandin 8-iso-F2α (1)	$C_{20}H_{34}O_5$	461/463	30

[a] $(M+^{107}Ag)^+/(M+^{109}Ag)^+$

is examined in solution. Spray solutions of the pure analytes in MeOH:H_2O (1:1) were analyzed in the negative ion mode for the free fatty acids. Typically, the ESSI limits of detection were of the same order of magnitude or an order of magnitude more sensitive, ~100 pg. This result is consistent with previous studies [31] which compared the DESI analysis to conventional ESI methods. Therefore, for conventional DESI analysis, an improvement of at least an order of magnitude is observed using silver ion attachment but there is no overall enhancement when compared to electrospray methods. However, unlike most ESI methods for the analysis of biosamples, DESI does not require sample clean-up or pretreatment.

The present results can also be compared to those of conventional methods of analysis for the same compounds investigated by GC, LC-ESI-MS and SIMS methods [47–50]. These techniques provide limits of detection for fatty acids and their esters within the ng/mL range. This is equivalent to the picogram detection limits observed for some of the analytes by DESI. However, prior to analysis by these methods, lipid analytes are typically derivatized to modify the functionality of the analytes to increase the sensitivity. Chromatographic methods also employ online concentration of the analytes to lower detection limits. Therefore, with the use of silver ions, the detection of these analytes by DESI gives comparable performance to conventional methods, while offering the additional advantages of rapid in situ analysis.

Investigation of competitive Ag$^+$ binding

To investigate the competitive binding of silver ion to particular fatty acids and prostaglandins, experiments were performed on a mixture of analytes (fatty acids, fatty acid derivatives and 8-iso-F2α). Analysis of a complex mixture (~3 ng of each analyte) yields prominent silver adducts due to pinolenic acid, arachidonic acid methyl and ethyl esters, and oleic acid as illustrated in Fig. 2. Pinolenic ethyl ester gave the most intense signal followed by arachidonic acid ethyl ester. These results, like those on the individual compounds, suggest that silver adduct formation favors the ester derivatives of the fatty acids. This affinity may be a result of the basic nature of the ester molecules when compared to the free acids. The data also suggest—although less strongly—that three olefin bonds may be the optimal number of unsaturated bonds for silver adduct formation although strong signals are also seen for olefins with more double bonds. Competitive binding does not directly correlate to the limit of detection as the detection limits for the arachidonic acid species were typically higher than those of the other fatty acid molecules but the results do suggest that improved binding occurs for molecules with multiple olefin bonds.

The results obtained during this DESI-MS study show interesting correlations with HPLC studies of fatty acids using silver salts [23, 26, 27]. Fatty acids elute during Ag-HPLC in the order of increasing number of *cis* double bonds and of decreasing chain lengths [23]. In the DESI

Fig. 2 Silver affinity determination by DESI analysis of a fatty acid and prostaglandin mixture (3 μg of each analyte) from teflon with a solvent spray of MeOH:H$_2$O (1:1) doped with 5.5 μg/mL of AgNO$_3$ using a Thermo Fisher Scientific LTQ of 3 μL samples (~7 mm^2 spot size)
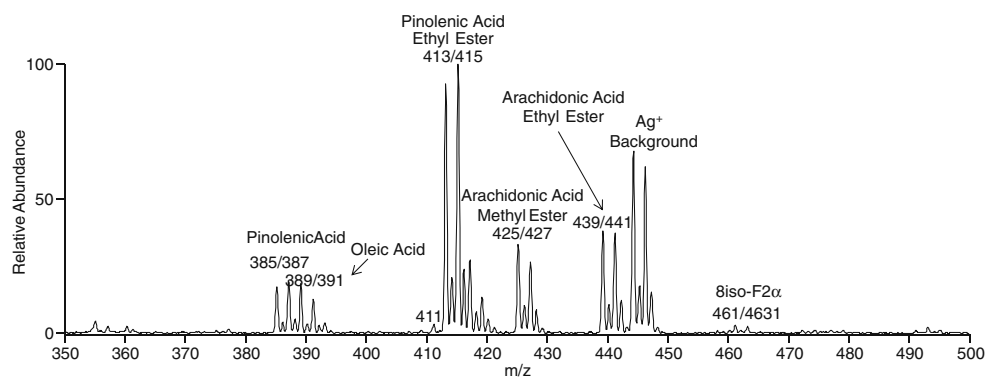
experiment, pinolenic acid and its ester ethyl derivative (C$_{18}$H$_{30}$O$_2$ and C$_{20}$H$_{34}$O$_2$) demonstrate a greater affinity for silver cationization than arachidonic acid and its derivatives (C$_{20}$H$_{32}$O$_2$, C$_{20}$H$_{24}$O$_2$, C$_{22}$H$_{36}$O$_2$, C$_{21}$H$_{34}$O$_2$). While arachidonic acid has one more *cis* olefinic bond, the chain is longer, decreasing its affinity when compared to pinolenic acid. In addition, further investigation into the minimized energy of the fatty acid structures suggests that pinoleneic acid as opposed to others like arachidonic acid may exhibit a "bay region" [24, 25] which is known to be highly favorable for silver adduct formation in the gas phase. Pinolenic acid, unlike the other fatty acids, does not only consist of olefins separated by –CH$_2$– but also –CH$_2$CH$_2$– which may lead to the formation of a bay region.
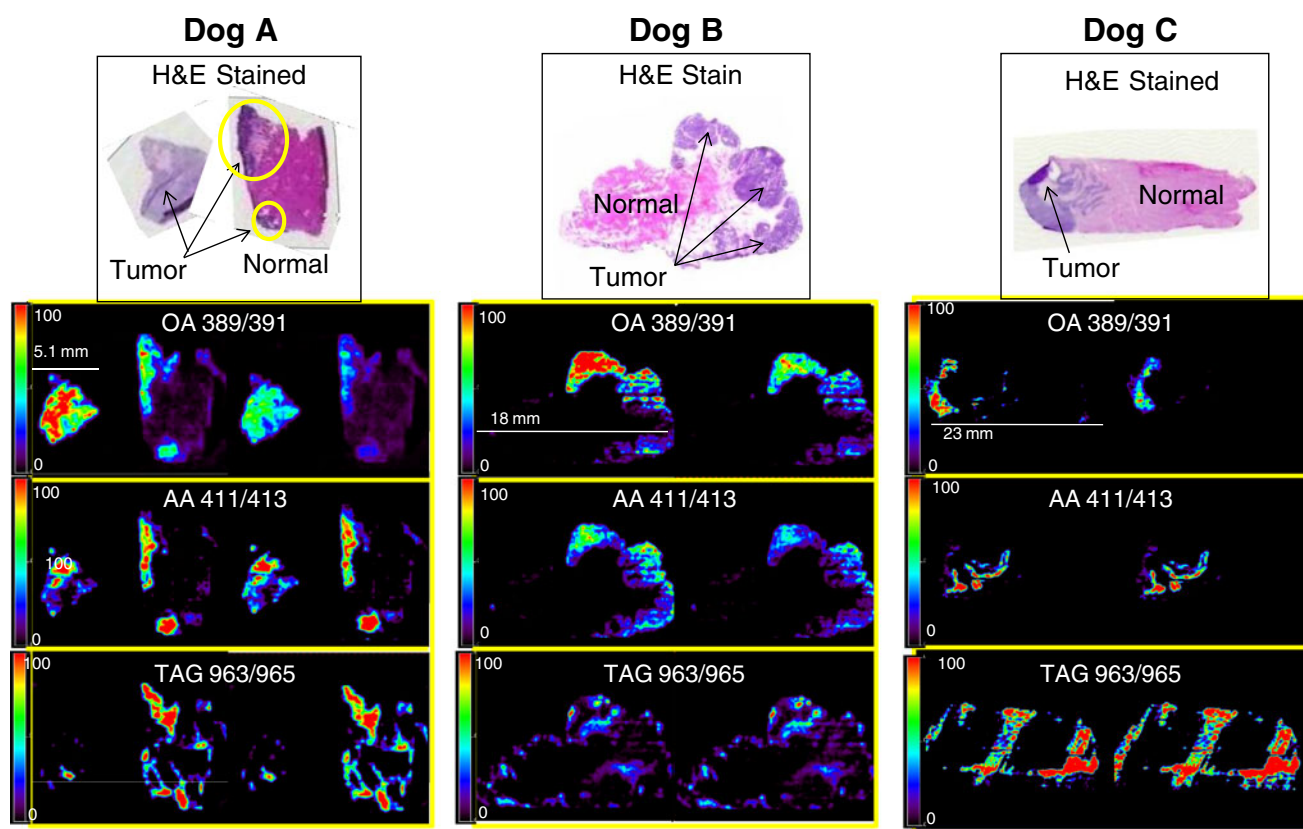

Fig. 3 Canine bladder tissue analysis by DESI-MS imaging of tissue samples from three different dog breeds using a silver ion as spray solvent highlighting the differences between normal and tumor sections for silver adducts of fatty acids (oleic acid *m/z* 389/391 18:1^{107}Ag/18:1^{109}Ag, arachidonic *m/z* 411/413 20:4^{107}Ag/20:4^{109}Ag), and a triacylglyceride (*m/z* 963/965). The images were acquired in the positive ion mode using ACN doped with 5.5 μg/mL AgNO$_3$ using a Thermo Fisher Scientific LTQ. Images of (M+^{107}Ag)$^+$/(M+^{109}Ag)$^+$ adducts are presented on the *left and right*, respectively, for each analyte corresponding to the two images for each analyte. *OA* oleic acid, *AA* arachidonic acid, *TAG* triacylglyceride

Ag$^+$ ion complexes and canine bladder tissue images

Cancerous and normal canine bladder tissue samples were imaged in three different canine models to assess the possible usefulness of silver ion cationization for detection of compounds present in a complex matrix. Using a silver-doped solvent spray, images of silver adducts were found to distinguish the tumor regions from normal tissue sections as illustrated in Fig. 3. Hematoxylin and eosin (H&E) stains are provided for comparison. The dark blue/purple regions denote the cancerous regions of the tissue samples. The fatty acid Ag$^+$ ion DESI images displayed allow ready distinction of the cancerous regions from normal regions for the three canine samples. Common ions were observed among the tissue samples but at different relative signal intensities. Therefore, each image has been normalized for the selected ion image of interest.

The compounds detected were confirmed through tandem analysis and are primarily fatty acids, details follow below. These tissues were studied previously in both the positive and negative ion modes using a conventional DESI solvent spray (ACN:H$_2$O, 1:1) [45]. The same fatty acids that were observed in the negative ion mode in the conventional solvent system are observed in the positive ion mode using the silver-doped spray. In the previous study, the positive ion mode images were limited to the monitoring of phospholipids.

Oleic acid (m/z 389/391), confirmed via tandem MS analysis, was a dominant indicator of the tumor versus normal tissue sections for all of the canine samples. It was also the dominant fatty acid observed in the negative ion mode of the previous study [45]. Since only three different canine samples are investigated, no biological conclusions can be drawn but the results are consistent with conventional DESI imaging data.

Although confirmed via tandem analysis, the ^{107}Ag and ^{109}Ag ion images for oleic acid are not identical as they should be, suggesting that there is overlap of the signal due to an additional fatty acid, linoleic acid. Confirmation of this overlap was achieved by performing tandem MS analysis on each ion (linoleic acid m/z 387/389 and oleic acid m/z 389/391) and derivation of the theoretical profile as summarized in Fig. 4. MS/MS of m/z 389 provided evidence of both ^{107}Ag from oleic acid and ^{109}Ag from linoleic acid. The overlap profile was consistent among the three different canine tissue samples and explains why the ion images do not simply correlate with silver isotopes. In cases where there is no overlap of the Ag$^+$ signals, the ^{107}Ag and ^{109}Ag images are essentially identical (1:1) as demonstrated for arachidonic acid (AA 411/413 in Fig. 2).

Other ions observed that were not reported in the previous study include triacylglycerides (TAGs) in the upper mass range (m/z>900). These biomolecules have not previously been detected in DESI images in either the

Fig. 4 Confirmation of the linoleic and oleic acid profiles by derivation of the theoretical profile and MS^n analysis of the ions of interest (linoleic acid m/z 387/389 and oleic acid m/z 389/391). MS^n of m/z 389 illustrated evidence of both ^{107}Ag from oleic acid and ^{109}Ag from linoleic acid. Mass spectra were obtained from DESI mass analysis of a tumor section of canine tissue
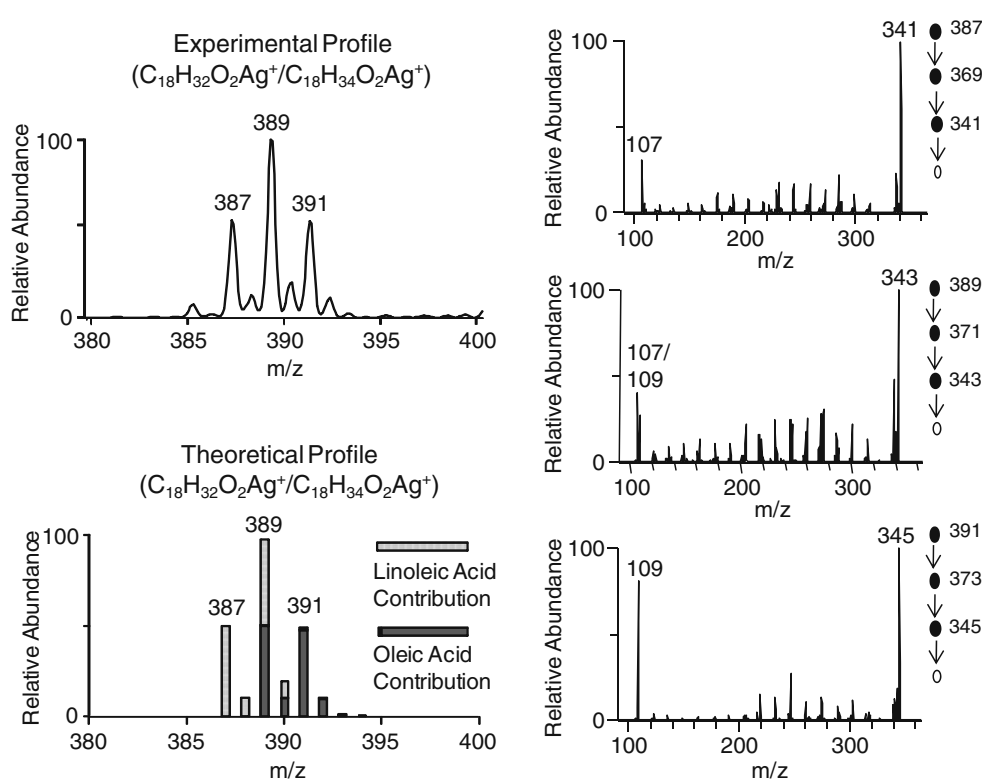
positive or negative ion modes as they do not have an ionizable head group as do phospholipids. However, the affinity for silver to these molecules is increased due to the olefin bonds. Tandem MS analysis of a TAG detected at m/z 963/965 resulted in fragmentation by losses of 284 Da and 256 Da corresponding to oleic acid and palmitic acid derivatives, respectively. Based on the Nature Lipid Maps database (freeware, http://www.lipidmaps.org) and tandem MS analysis of the TAG, it is likely TG(16:1(9Z)/18:1(9Z)/18:1(9Z))[iso3]. Unlike the fatty acids, the TAG is distributed throughout the entire tissue sample and does not readily allow distinction of the tumor from the normal regions.

Isomer distinction

The group of fatty acids evaluated included three sets of isomers: oleic acid (9Z-$C_{18}H_{34}O_2$)/palmitoleic acid ethyl ester (9Z-$C_{18}H_{34}O_2$), linolenic acid ethyl ester (9Z,12Z,15Z-$C_{20}H_{34}O_2$)/pinolenic acid ethyl ester (5Z, 9Z, 12Z-$C_{20}H_{34}O_2$), and γ-linolenic acid (6Z, 9Z, 12Z-$C_{18}H_{30}O_2$)/α-linolenic acid (9Z,12Z, 15Z-$C_{18}H_{30}O_2$)/pinolenic acid (5Z, 9Z, 12Z-$C_{18}H_{30}O_2$). These isomers could be distinguished by tandem MS using collision-induced dissociation after silver ion attachment. MS^n experiments were performed on 30 ng of each analyte and the results are summarized in Fig. 5. Most of the isomers could be
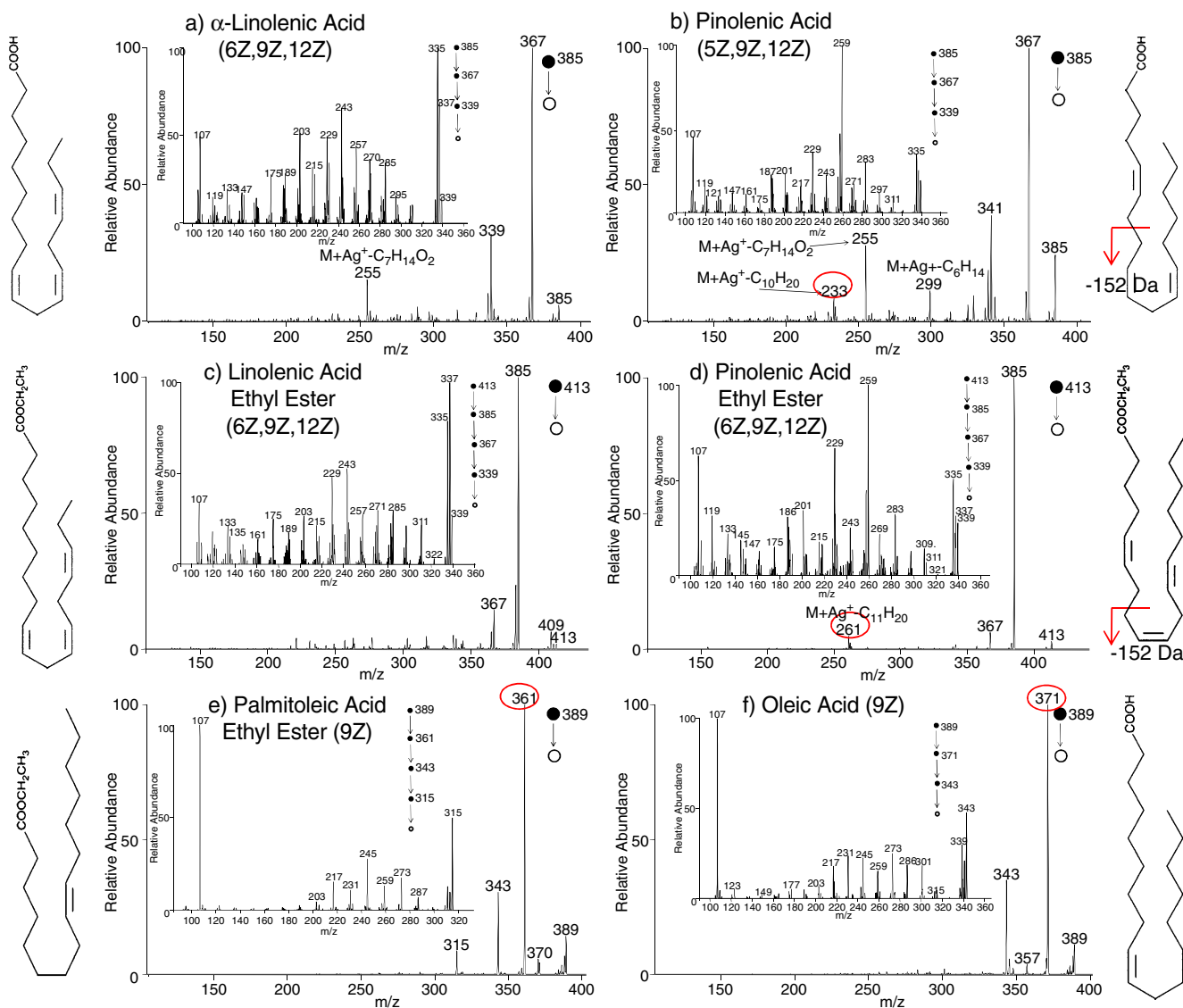
Fig. 5 Tandem DESI-MS using collision-induced dissociation to distinguish isobaric ions: a–b α-linolenic acid (6Z, 9Z, 12Z-$C_{18}H_{30}O_2$)/pinolenic acid (9Z,12Z, 15Z-$C_{18}H_{30}O_2$), c–d linolenic acid ethyl ester (9Z,12Z,15Z-$C_{20}H_{34}O_2$)/pinolenic acid ethyl ester (5Z, 9Z, 12Z-$C_{20}H_{34}O_2$), and (e–f)oleic acid (9Z-$C_{18}H_{34}O_2$)/palmitoleic acid ethyl ether (9Z-$C_{18}H_{34}O_2$); 30 ng of each analyte was analyzed from teflon with a solvent spray of MeOH:H_2O (1:1) doped with 5.5 µg/mL of AgNO$_3$ using a Thermo Fisher Scientific LTQ of 3 µL pipetted samples (~7 mm^2 spot size)

distinguished using MS^2 analysis but MS^4 or MS^5 data were typically acquired for further confirmation as observation of the silver ion fragment allowed elucidation of the olefin bond location. Typical fragment ions observed resulted from ethylene (28 Da) and water (18 Da) losses. The ethyl ester derivatives could be readily distinguished from the free fatty acids as the ethyl esters yielded a dominant ethylene loss fragment ion while the free fatty acids yielded a dominant water loss fragment ion associated with the carboxylic functionality. This assisted in distinguishing the structural isomers palmitoleic acid ethyl ester from oleic acid.

Beyond distinguishing esters from free fatty acids, ions with varying olefin locations were distinguished. For instance, α-linolenic acid was clearly distinguished from pinolenic acid in both the free fatty acid and ethyl ester forms. In the case of the free fatty acids, MS^5 analysis was needed to conclusively distinguish the isomers. The MS^5 spectra yielded different profiles of the unsaturated backbone of the molecules due to the difference in olefin location. The ethyl ester derivatives could be distinguished using simple MS/MS analysis as pinolenic acid ethyl ester yielded a unique fragment ion at m/z 261 corresponding to the loss of $C_{11}H_{20}$. This fragment structurally corresponds to the C8–C18 unsaturated carbon chain of pinolenic acid ethyl ester which includes the last two olefin bonds. A similar loss was also observed for the free fatty acids as well.

Isomer differentiation based on the location of the olefin bond and tandem MS analysis to confirm the identity of the analytes has implications for reaction monitoring (MS/MS) based DESI imaging. While single ion monitoring images can be obtained successfully by DESI, there is no conclusive structural evidence regarding the nature of the analytes. The ability to record images by detecting key fragments of specific analytes should provide simultaneous DESI images with structural confirmation. This will aid in the imaging of analytes within adduct matrices like tissues where there could be several isobaric ions. Further, this may help detect ions which are typically suppressed by co-located but more concentrated analytes.

Conclusions

Silver ion containing DESI spray solvents facilitate the analysis of unsaturated molecules, including biologically relevant fatty acids, fatty acid esters, and prostaglandins, by improving their detection limits by an order of magnitude when compared to conventional DESI. This simple experiment therefore gives, for appropriate compounds, similar sensitivity to that achieved by electrospray ionization. Correlations with the number of olefinic groups were sought through competitive binding studies but only the general favorability of silver ion binding to polyolefins was demonstrated. Proof of principle of the usefulness of silver cationization in DESI tissue imaging is provided and the first acylglyceride images are reported.

Given the affinity of silver ions to various olefin systems, there are other fields where silver spray solutions might also be useful. They include petroleum exploration and analysis given the importance of unsaturated and aromatic species in these samples and polynuclear aromatic hydrocarbons in the environment.

References

1. Watson AD (2006) Thematic review series: systems biology approaches to metabolic and cardiovascular disorders. Lipidomics: a global approach to lipid analysis in biological systems. J Lipid Res 47:2101–2111
2. Leung CL, Pang Y, Shu C, Goryunov D, Liem RKH (2007) Alterations in lipid metabolism gene expression and abnormal lipid accumulation in fibroblast explants from giant axonal neuropathy patients. BMC Genet 8:1–12
3. Byrdwell WC (2010) Dual parallel mass spectrometry for lipid and vitamin D analysis. J Chromatogr A 1217:3992–4003
4. Han X (2010) Multi-dimensional mass spectrometry-based shotgun lipidomics and the altered lipids at the mild cognitive impairment stage of Alzheimer's disease. Biochim Biophys Acta 1801:774–783
5. Shevchenko A, Simons K (2010) Lipidomics: coming to grips with lipid diversity. Nat Rev Mol Cell Biol 11:593–598
6. Chen HW, Gamez G, Zenobi R (2009) What can we learn from ambient ionization techniques? J Am Soc Mass Spectrom 20:1947–1963
7. Van-Berkel GJ, Pasilis SP, Ovchinnikova O (2008) Established and emerging atmospheric pressure surface sampling/ionization techniques for mass spectrometry. J Mass Spectrom 47:1161–1180
8. Venter A, Nefliu M, Cooks RG (2008) Ambient desorption ionization mass spectrometry. Trends Anal Chem 27:284–290
9. Cooks RG, Ouyang Z, Takats Z, Wiseman JM (2006) Ambient mass spectrometry. Science 311:1566–1570
10. Takats Z, Wiseman JM, Gologan B, Cooks RG (2004) Mass spectrometry sampling under ambient conditions with desorption electrospray ionization. Science 306:471–473
11. Fordham PJ, Chamot-Rooke J, Giudice E, Tortajada J, Morizur JP (1999) Analysis of alkenes by copper ion chemical ionization gas chromatography/mass spectrometry and gas chromatography/tandem mass spectrometry. J Mass Spectrom 34:1007–1017
12. Lequere JL, Sebedio JL, Henry R, Couderc F, Demont N, Prome JC (1991) Gas chromatography-mass spectrometry and gas chromatography-tandem mass spectrometry of cyclic fatty acid monomers isolated from heated fats. J Chromatogr Biomed Appl 562:659–672
13. Peake DA, Huang SK, Gross ML (1987) Iron(I) chemical ionization for analysis of alkene and alkyne mixtures by tandem sector mass spectrometry or gas chromatography/Fourier transform mass spectrometry. Anal Chem 59:1557–1563
14. Bell SE, Ewing RG, Eiceman GA, Karpas Z (1994) Atmospheric pressure chemical ionization of alkanes, alkenes, and cyclo-alkanes. J Am Soc Mass Spectrom 5:177–185

15. Le Quere JL, Semon E, Lanher B, Sebedio JL (1989) On-line hydrogenation in GC-MS analysis of cyclic fatty acid monomers isolated from heated linseed oil. Lipids 24:347–350

16. Eiceman GA, Fuavao VA, Doolittle KD, Herman CA (1982) Determination of prostaglandin precursors in frog tissue using selected-ion monitoring in gas-chromatographic mass spectromic analysis. J Chromatogr 236:97–104

17. Le Grandois J, Marchioni E, Zhao M, Giuffrida F, Ennahar S, Bindler F (2009) Investigation of natural phosphatidylcholine sources: separation and identification by liquid chromatography-electrospray ionization-tandem mass spectrometry (LC-ESI-MS2) of molecular species. J Agr Food Chem 57:6014–6020

18. Yin H, Porter NA (2007) Identification of intact lipid peroxides by Ag+ coordination ion-spray mass spectrometry (CIS-MS). Methods Enzymol 433:193–211

19. Nomiya K, Kondoh Y, Nagano H, Oda M (1995) Characterization by electrospray ionization (ESI) mass spectrometry of an oligomeric, anionic thiomalato-silver(I) complex showing biological activity. J Chem Soc Chem Commun 1679–1680

20. Choi SS, Ha SH (2007) Influence of silver salt types on formation of silver cluster ions in MALDI with DHB as matrix, kor. Chem Soc 28:2508–2510

21. Choi SS, Ha SH (2008) Influence of sample preparation method and silver salt types on MALDI-TOFMS analysis of polybutadiene. Macromol Res 16:108–112

22. Grade H, Winograd N, Cooks RG (1977) Cationization of organic molecules in secondary ion mass spectrometry. J Am Chem Soc 99:7725–7726

23. Nikolova-Damyanova B (2009) Retention of lipids in silver ion high-performance liquid chromatography: facts and assumptions. J Chromatogr A 1216:1815–1824

24. Hand OW, Winger BE, Cooks RG (1989) Enhanced silver cationization of polycyclic aromatic hydrocarbons containing bay regions in molecular secondary ion mass spectrometry. Biomed Environ Mass Spectrom 18:83–85

25. Ng KM, Ma NL, Tsang CW (1998) Cation-aromatic π interaction in the gas phase: an experimental study on relative silver (I) ion affinities of polyaromatic hydrocarbons. Rapid Commun Mass Spectrom 12:1679–1684

26. Momchilova S, Nikolova-Damyanova B (2003) Stationary phases for silver ion chromatography of lipids: preparation and properties. J Sep Sci 26:261–270

27. Nikolova-Damyanova B, Momchilova S (2002) Silver ion HPLC for the analysis of positionally isomeric fatty acids. J Liq Chromatogr Relat Technol 25:1947–1965

28. Muddiman DC, Brockman AH, Proctor A, Houalla M, Hercules DM (1994) Characterization of polystyrene on etched silver using ion-scattering and X-ray photoelectron-spectroscopy—correlation of secondary-ion yield in time-of-flight SIMS with surface coverage. J Phys Chem 98:11570–11575

29. Nicola AJ, Muddiman DC, Hercules DM (1996) Enhancement of ion intensity in time-of-flight secondary-ionization mass spectrometry. J Am Soc Mass Spectrom 7:467–472

30. Bereman MS, Muddiman DC (2007) Detection of attomole amounts of analyte by desorption electrospray ionization mass spectrometry (DESI-MS) determined using fluorescence spectroscopy. J Am Soc Mass Spectrom 18:1093–1096

31. Garcia-Reyes JF, Jackson AU, Molina-Diaz A, Cooks RG (2009) Desorption electrospray ionization mass spectrometry for trace analysis of agrochemicals in food. Anal Chem 81:820–829

32. Manicke NE, Kistler T, Ifa DR, Cooks RG, Ouyang Z (2009) High-throughput quantitative analysis by desorption electrospray ionization mass spectrometry. J Am Soc Mass Spectrom 20:321–325

33. Wiseman JM, Ifa DR, Zhu Z, Kissnger CB, Manicke NE, Kissinger PT, Cooks RG (2008) Ambient molecular imaging by desorption electrospray ionization mass spectrometry. Nat Protoc 3:517–524

34. Kennedy JH, Wiseman JM (2010) Direct analysis of salvia divinorum leaves for salvinorin a by thin layer chromatography and desorption electrospray ionization multi-stage tandem mass spectrometry. Rapid Commun Mass Spectrom 24:1305–1311

35. Nyadong L, Late S, Green MD, Banga A, Fernandez FM (2008) Direct quantitation of active ingredients in solid artesunate antimalarials by noncovalent complex forming reactive desorption electrospray ionization mass spectrometry. J Am Soc Mass Spectrom 19:380–388

36. Costa AB, Cooks RG (2007) Simulation of atmospheric transport and droplet—thin film collisions in desorption electrospray ionization. Chem Commun 38:3915–3917

37. Costa AB, Cooks RG (2008) Simulated splashes: elucidating the mechanism of desorption electrospray ionization mass spectrometry. Chem Phys Lett 464:1–8

38. Venter A, Sojka PE, Cooks RG (2006) Droplet dynamics and ionization mechanisms in desorption electrospray ionization mass spectrometry. Anal Chem 78:8549–8555

39. Cotte-Rodriguez I, Cooks RG (2006) Non-proximate detection of explosives and chemical warfare agent simulants by desorption electrospray ionization mass spectrometry. Chem Commun 28:2968–2970

40. Ifa DR, Wiseman JM, Song QY, Cooks RG (2007) Development of capabilities for imaging mass spectrometry under ambient conditions with desorption electrospray ionization (DESI). Int J Mass Spectrom 259:8–15

41. Wu C, Ifa DR, Manicke NE, Cooks RG (2010) Molecular imaging of adrenal gland by desorption electrospray ionization mass spectrometry. Analyst 135:28–32

42. Wu C, Qian K, Nefliu M, Cooks RG (2010) Ambient analysis of saturated hydrocarbons using discharge-induced oxidation in desorption electrospray ionization. J Am Soc Mass Spectrom 21:261–267

43. Nyadong L, Green MD, De Jesus VR, Newton PN, Fernandez FM (2007) Reactive desorption electrospray ionization linear ion trap mass spectrometry of latest-generation counterfeit antimalarials via noncovalent complex formation. Anal Chem 79:2150–2157

44. Venter A, Cooks RG (2007) Desorption electrospray ionization in a small pressure-tight enclosure. Anal Chem 79:6398–6403

45. Dill AL, Ifa DR, Manicke NE, Costa AB, Ramos-Vara JA, Knapp DW, Cooks RG (2009) Lipid profiles of canine invasive transitional cell carcinoma of the urinary bladder and adjacent normal tissue by desorption electrospray ionization imaging mass spectrometry. Anal Chem 81:8758–8764

46. Takats Z, Wiseman JM, Gologan B, Cooks RG (2005) Electrosonic spray ionization. a gentle technique for generating folded proteins and protein complexes in the gas phase and for studying ion-molecule reactions at atmospheric pressure. Anal Chem 76:4050–4058

47. Devle H, Rukke EO, Naess-Andresen CF, Ekeberg D (2009) A GC–magnetic sector MS method for identification and quantification of fatty acids in ewe milk by different acquisition modes. J Sep Sci 32:3738–3745

48. Ingram JC, Bauer WF, Lehman RM, O'Connell SP, Shaw AD (2003) Detection of fatty acids from intact microorganisms by molecular beam static secondary ion mass spectrometry. J Microbiol Methods 53:295–307

49. Kurata S, Yamaguchi K, Nagai M (2005) Rapid discrimination of fatty acid composition in fats and oils by electrospray ionization mass spectrometry. Anal Sci 21:1457–1465

50. Chu XP, Zhao T, Zhang YY, Zhao AH, Zhou MM, Zheng XJ, Dan M, Jia W (2009) Determination of 13 free fatty acids in pheretima using ultra-performance LC-ESI-MS. Chromatographia 69:645–652